Chapter

Polarization of Electrospun PVDF Fiber Mats and Fiber Yarns

Harshal Gade, Sreevalli Bokka and George G. Chase

Abstract

Electrospun fibers are of interest in a number of applications due to their small size, simplicity of fabrication, and ease of modification of properties. Piezoelectric polymers such as Polyvinylidene Fluoride (PVDF) can be charged when formed in the electrospinning process. This chapter discusses fabrication of PVDF fiber mats and fiber yarns and the measurement of their charge using a custom-made Faraday bucket. The results show the measured charge per mass of fiber mats was greater than the values measured for the yarns of the same mass. The measured charges may be related to both mass and external surface areas of the mats and yarn samples. It was observed the area/mass ratios of the fiber yarns were more than 30% less than the fiber mats.

Keywords: PVDF, Faraday bucket, electrospinning, yarns, fibers

1. Introduction

In recent years, nanotechnology has been used to develop novel materials including nano and submicron scaled materials such as nanorods, nanofoams, nanotubes, nanofilms, and nanofibers. These materials find use in various industrial applications and are the topics of many contemporary academic research efforts. Of these materials, the polymer electrospun fibers have found broad uses for catalysis, drug delivery, semiconductors and filtration [1–3].

Many polymers have been electrospun into nonwoven fiber mats. The polymer materials can have intrinsic piezo, thermal, and mechanical properties. When the polymers are formed into fiber structures such as thin mats, the high porosities and high specific surface areas of the mats can enhance the mat structural properties compared to similar mats of microfibers. The material and structural properties of these mats are ideally suited for filter media for air filtration and face masks.

Less common in the literature are discussions of the fabrication of yarns from electrospun fibers. The fabrication of yarns requires a mechanical method to entangle and interlock the intrinsic fibers, often by twisting, to form a self-supporting assembly of the fibers of an overall cylindrical shaped structure that can be characterized by a structure diameter.

Prior to electrospinning, the submicron fibers were often synthesized by techniques such as drawing, templating, solution casting, and phase separating. Most of these techniques had shortcomings including deformation failures, inability to produce continuous fibers, inability to scale-up, low production rates, or significant by-product wastes. The electrospinning method overcomes some of these shortcomings, and because of its simplicity, is a highly popular synthesis method.

Electrospinning is well-documented, established, and cost-effective, and is applied commercially. **Figure 1** shows numbers of publications, by publication year, as determined from the Scifinder ™ data base for the past 25 years. The plot shows a steady rise in numbers of papers since about 2000 when Reneker [4] published a seminal paper on electrospinning. The data search was conducted in August 2020 hence the final year was incomplete.

Electrospinning has been used to spin fibers for a wide range of polymers. One of these polymers, polyvinylidene fluoride (PVDF), is well known for its electrical properties. PVDF exhibits five known crystalline phases- α, β, γ, δ and ε. Amongst them, the β-phase has the highest permanent dipole moment due to its trans, TTT, planar zig-zag configuration. The β-phase is considered most responsible for the piezoelectric response obtained from the PVDF materials. A goal of enhancing the beta-phase contents in PVDF materials is an ongoing research pursuit [5, 6].

Electrospun fibers have been used as electrets in several applications. Electrets have a surface charge which can be exploited in capturing charged particles. Nanofibers can be converted into electrets by various methods such as corona discharging, surface fluorination and nafion functionalization. Several research groups developed custom made bench-scale procedures to produce polarized fibers which involved simultaneous stretching, heating and electrical poling. Similarly, Lolla *et al.* [6, 7] produced polarized PVDF fiber mats and tested them for aerosol filtration. The polarized fibers were observed to have higher surface charges, better capture efficiencies and lower pressure drops compared to as-spun fibers. The study was limited by measurement of localized surface potential via a hand-held electrostatic field meter [6]. **Table 1** lists several instruments reported in literature used to measure surface potential and charge. All of these instruments make localized measurements (do not measure properties over a large area of a mat) and may be impractical to use for production scale processes due to complexity and cost of operations. Measurements of the surface potential or electrical field are related to electrical charges but methods to calculate charges from the measurements are not always apparent.

Gade *et al.* [12] fabricated a custom-made Faraday bucket and a procedure to calculate the charges of fiber mat samples. The Faraday bucket overcomes some limitations or challenges of using the methods listed in **Table 1**, namely: it is non-destructive, measures large sample sizes, is easy to scale-up, and has a tractable mathematical model to convert voltage to charge value. In this chapter, the Faraday

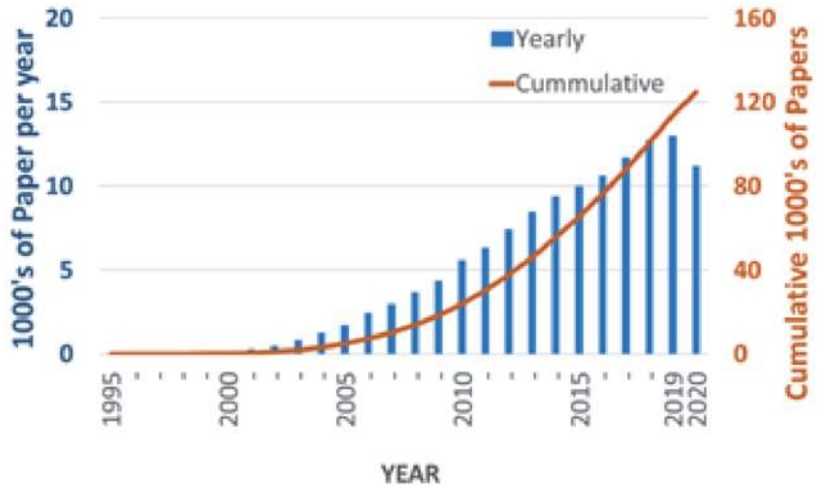

Figure 1.
Number of publications on "electrospinning" versus year of publication.

bucket is used to measure and compare charges between electrospun fiber mats and electrospun (continuous twisted fiber) yarns. Layers of fibers mats and yarns were stacked together to explore whether the Faraday bucket was more sensitive to bulk (mass) charge or more sensitive to surface charge. The charges on polarized fibers and yarns are also compared.

Many publications discuss methods to charge fibers or to modify fibers surfaces (with coatings or additives such as carbon nanotubes) to enhance performances of fiber filter media. The subject matter is broad, and the numbers of publications are too numerous for a complete list. **Table 2** lists a sample of some of the publications.

The electrospinning processes typically produce nonwoven, randomly oriented, fiber mats. These fiber mats typically have low mechanical strength (compared to microfiber mats). The electrospinning processes have a low mass production rates per nozzle that limits commercial applications from an economic standpoint. Researchers have studied various approaches to increase the mass production by increasing the number of electrospinning jets in the process [25, 26]. To overcome some of the limitations, researchers have studied electrospun yarns to improve the alignment of fibers and to increase the mechanical strength. Production of highly twisted PVDF – HFP electrospun fiber yarns using a novel ring collector was reported by Shuakat *et al.* [27]. Afifi *et al.* [28] and Teo *et al.* [29] studied methods to continuously produce electrospun yarns. In this chapter the yarns were produced by twisting and drawing the fibers in flight and the twisted yarn were wound onto

Researcher	Instrument	Materials tested	Reference
Collins *et al.*	Scanning Probe microscopy	Various dielectric surfaces	[8]
Du *et al*.	Kelvin Probe force microscopy (open and closed loop techniques)	Single and multi-layer graphene structures	[9]
Takahashi and Yoshita	Inversion algorithmic methods	DC basin-type insulator	[10]
Fatihou *et al*.	Electrostatic voltmeter	Electrospun PVDF nanofibers	[11]
Lolla *et al*.	Electrostatic field meter	Polarized electrospun nanofibers	[6]

Table 1.
List of instruments and materials tested.

Researcher(s)	Description	Reference(s)
Fredrick Brown	Fundamental physics of electrical and charge effects on filter performance	[13, 14]
Choi *et al*.	Aluminum coatings applied to micro and nanoscale fibers, modified surface charge to control filter performance	[15]
Romay *et al.* Walsh *et al.* Wang *et al.*	Quasi-permanent charges on dielectric polymer fibers	[16–19]
Liu *et al.* Khalid *et al.* Jing *et al.*	Filters made of highly polar polymer fibers showing high binding affinity to fine particulate matter in aerosols	[20–22]
Li *et al.*	Fibrous filters hybridized with carbon nanotubes (CNT) exhibiting slip flow effects at the CNT surfaces	[23, 24]

Table 2.
A sampling of literature on topics of fiber surface charge, fiber coatings, and additives.

a spool, which differs from typical electrospinning equipment that collect the fiber mats on a solid grounded surface. The resulting yarns had lengths up to tens of meters long and exhibited mechanical properties different from the electrospun mats.

2. Materials and methods

2.1 Materials

Electrospinning solutions were prepared by dissolving PVDF powder (Arkema Inc., Exton, PA, USA, Kynar® 761 grade resin with molecular weight of 500,000 g/gmol and density of 1.78 g/m^3) in co-solvents N-N-Dimethylformamide (DMF) and acetone (Sigma Aldrich, St. Louis, MO, USA). These materials were used in making the solutions without further purification.

2.2 Preparation of as-spun solutions

Observations while electrospinning the fiber mats and yarns showed different fiber diameters were obtained for the two processes likely due to variations in setup geometries and electric field strengths. By trial and error in varying solution concentrations, appropriate solution concentrations for the two processes were determined to produce fibers with diameters of 1200 nm for both processes. The comparisons of charges and properties discussed in the experiments below were obtained for fibers with these diameters.. Electrospinning solutions for producing fiber mats were prepared with 18%wt PVDF polymer by mixing the polymer with 50:50 wt.% blended DMF and Acetone solvents. The PVDF powder was added to mixture of solvents and heat-stirred for half an hour at 70 °C to attain a clear homogenous mixture. For production of fiber yarns, a 13 wt% PVDF polymer solution was prepared by mixing Acetone and N, N-Dimethylformamide (DMF) solvents at 1:1 ratio. This mixture was heated on a hot plate at 70 °C for 20 min to attain a clear homogenous mixture.

2.3 Electrospinning set-ups and mechanism

The fiber mats were synthesized by using a typical single-needle electrospinning setup as shown in **Figure 2.** The polymer solutions were loaded into 5 ml plastic syringes and fed by syringe pump (NE-1000, New Era Pump Systems, Inc., Farmingdale, NY). The metallic needles were charged by high voltage power supplies (ES30P-5 W, Gamma High Voltage Research, Ormond Beach, FL) to generate potential differences between the collector and the needle. The fiber mats were collected on rotating cylindrical drum collectors covered with 30 cm × 30 cm sheets of grounded aluminum foil. The fiber mats were electrospun for varying times to create mats of basis weights of 10, 20, 30, 40 and 50 g/m^2. In the experiments involving stacked layers of mats, all of the layers were formed of mats of 20 g/m^2 basis weights. The electrospinning conditions are listed in **Table 3**.

Figure 3 shows the experimental setup used to generate the electrospun yarn and is similar to setups reported in literature [28, 30]. The setup consisted of fiber spinning and yarn winding sections. In the fiber spinning section, a metallic conical-shaped funnel collector was connected to the motor and controller. The syringe pump and power supply were used to electrospin the polymer solution at a flowrate of 4 - 5 ml/hr. A potential difference of 10 – 20KV was applied between the

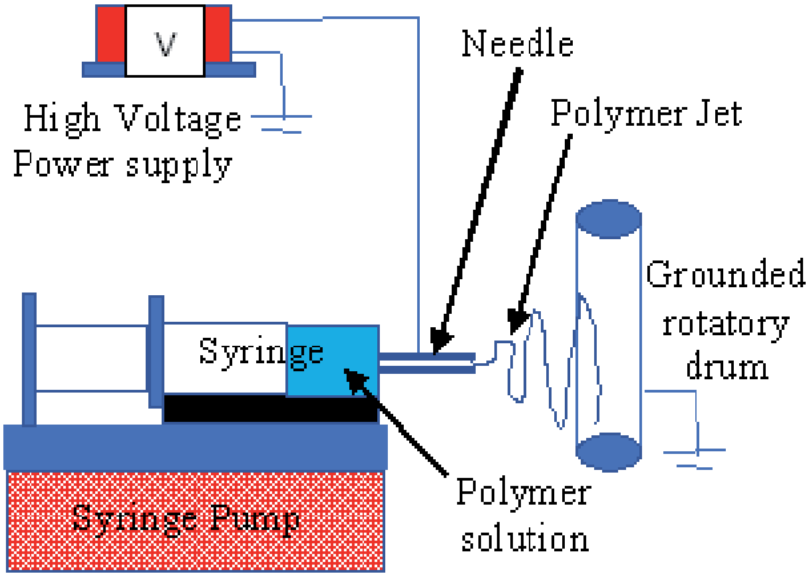

Figure 2.
Schematic of electrospinning set-up.

PVDF (wt.%)	DMF – Acetone mass ratio	Tip to Collector Distance (cm)	Applied Potential (kV)	Flow Rate (ml/hr)	Avg. Fiber Diameter (nm)	Standard Deviation (nm)	Drum Rotation Rate (rpm)
18	1:1	20	27	5	1139	654	30

Table 3.
Electrospinning conditions and fiber diameter data.

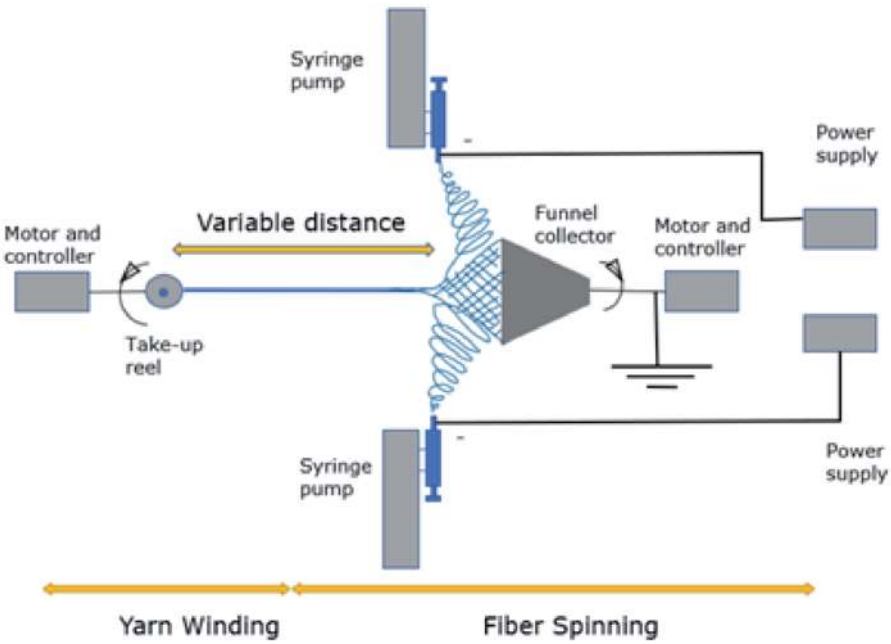

Figure 3.
Illustration of fiber yarn setup.

metal needles and the collector with an 8 cm distance between the needles and the edge of the collector.

Charged polymer jets launched from drops of polymer solution at the tips of the needles and followed the electric field gradient towards the wide neck of the conical-shaped collector. Once a substantial mat of fibers collected over the open end of the collector, the center of mat was hooked onto a wire and pulled to stretch the mat into the shape of an inverted cone.

The metal collector was rotated by the motor to twist the fiber structure into a twisted continuous yarn. The yarn gradually increased in length and was stretched and attached to the take-up reel for collection onto a spool. The rotation speeds of the metal collector and the take-up reel were adjusted by trial and error to produced yarns of uniform twist and uniform outer diameter.

In the case of electrospun mats, replicate samples were obtained at consistent basis weights by adjusting the time of fiber accumulation on the mats, so that the resulting fiber mat had uniform thickness and mass over the area of the sample. But in the case of fiber yarns a suitable length of sample was considered from each replicate run and compared for consistency by comparing the mass to length ratio of each sample. Results showed ±3% variation in mass/length for each of sample used in these experiments.

2.4 Polarization procedure

Mats and yarns were polarized by the treatments described below. The treatments were not applied to stacked layers of mats in the layered mat experiments described later. **Figure 4** (a) shows a photograph of the sample holder made of PTFE (Teflon®) for the main frame, brass bars for the clamps, and thin aluminum plates for the electrodes. The PTFE was chosen over other materials as it was easy to machine and had many desired properties such as low electrical conductivity, low dielectric constant, and relatively high melt temperature. **Figure 4** (b) shows the sample holder inside of a Fischer Scientific iso-temp oven. The aluminum plates were 19 cm × 11 cm and 1 mm in thickness. One aluminum plate was grounded and

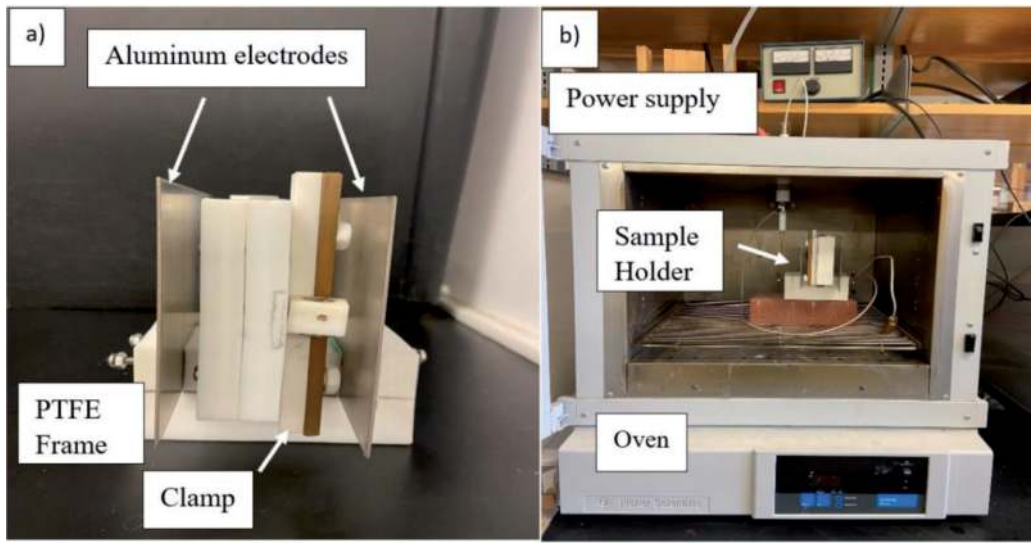

Figure 4.
(a) End view of fabricated sample holder showing the two planar electrodes used to apply the electric field for poling the sample. (b) Photo of sample holder inside of oven and high voltage power supply for charging the electrode above the oven.

the other was electrically charged to produce an electric field between the plates of 2.5 kV/cm. The distance between the electrodes was 6 cm. The fiber mat samples and yarn samples were placed in the holder to perform all polarization treatments including simultaneous heating, stretching and electrical poling.

Heat treatments were applied to change the sample temperature from room temperature to 150 °C with a temperature ramp-up rate of about 10C per min up to the soak temperature (150 C). The sample was held at the soak temperature for 5 minutes and then allowed to cool at a temperature ramp-down at rate of about 10C/min. The oven did not have ramp-rate control, so the ramp rates are estimates based on observed temperature readings.

The electric field poling was applied at field strength of 2.5 kV/cm during the heating of the oven. The poling started at the same time as the oven and stopped when the oven was turned off at the end of the soak time.

Uniaxial stretched mats and yarns were obtained by clamping the mats and yarns into the holder positioned parallel to and between the aluminum electrodes. The moveable clamp was moved to create a 10% stretch of the samples. The stretch time of the sample started when the sample was placed in the holder and stretched. The stretch time included time to place the holder into the oven, temperature ramp-up, temperature soak, temperature ramp-down, time to remove the holder, and ended when the sample was removed from the stretching mechanism in the holder, for a total of about 52 min. The as-spun and polarized samples were stored in the static shielding bags immediately after fabrication to avoid any dissipation of ions or charge.

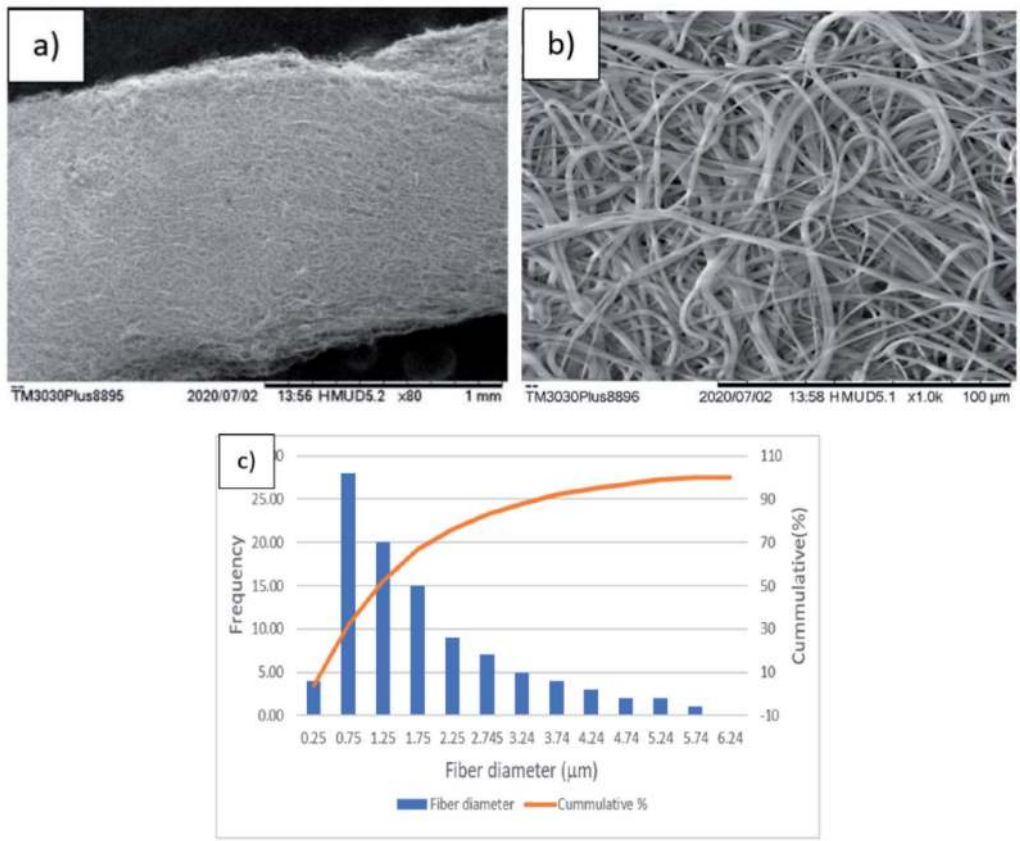

Figure 5.
SEM images of (a) fiber yarn and (b) fibers as seen on the surface of the fiber yarn with average fiber diameter of 1139 nm ± 654 nm, and average fiber yarn diameter of 900 µm ± 300 µm and c) fiber size distribution curve.

2.5 Characterization methods

The morphology characteristics of the electrospun fiber mats and yarns were observed using a scanning electron microscopy (SEM, TM3000 and TM3030 Plus, and Hitachi, Japan). SEM images were analyzed by FibraQuant 1.3 software (nano Scaffold Technologies, LLC, Chapel Hill, NC) to measure the fiber diameter distributions. **Figure 5** shows SEM images and fiber size distributions for PVDF fibers and yarns. Electric charges on the fiber mat were measured using a Faraday Bucket. A detailed description of the Faraday Bucket is given in reference [12]. The fiber mats were cut to the size needed for the measurement (4 cm by 4 cm) otherwise the measurements were non-destructive. Based on the electrostatic principles, as a sample lowered into the interior of the Faraday Bucket, the inner metallic "bucket" acquired an electric potential that was detected as a change in voltage relative to the surroundings (ground). By an appropriate circuit model of the Faraday bucket the measured potential was converted to charge.

Fiber yarns produced using setup in **Figure 3** were characterized as-spun and after polarization discussed in Section 2.4. The as-spun and polarized yarn samples were wrapped on a 'U' shaped copper wire and lowered into the Faraday bucket for measurement. The calculated charges were normalized with respect to mass of sample as discussed by Gade *et al.* [12]. The influence of U-shaped wire holding the yarn on the measured charge was found to be negligible when the wire without yarn was lowered into the Faraday bucket and produced zero measured voltage.

3. Results and discussions

3.1 Effect of stacking of fiber mats on charge measurement

Evaluation of the effects on charge measurments of stacked of mats was conducted only with as-spun mats (not with polarized mats). The purpose of this was to assess whether the Faraday bucket measurements were more sensitive to surface area or to mass of the samples.

Figure 6a shows a photograph of a single 4 × 4 cm fiber mat. **Figure 6b** shows five as-spun mats stacked on top of each other. All mats were cut to size 4 cm × 4 cm and had a 1 × 1 cm tab at one edge. **Figure 6c** shows a bar chart of calculated charges per unit mass of individual and stacked layer samples. The measurements of the five individual samples are labeled as 1 to 5. The stacked samples are labeled A to D where A was formed by stacking the mats 1 + 2 (i.e., individual mats 1 and 2 stacked), B was three mats 1 + 2 + 3, C was four mats 1 + 2 + 3 + 4, and D was five mats 1 + 2 + 3 + 4 + 5.

All the single mats in **Figure 6c** had approximately the same measured charges of about 130 nC/g. All the mats had the same basis weight (20 g/m^2), hence had the same masses.

If the Faraday bucket detected charge in bulk (i.e. per mass) then stacking the mats should not show a difference in charge/mass. If the Faraday bucket detected charge based on charge on the external mat surface area, and the charges of the mats do not transfer between the mats, then we would expect the measured charge/mass to decrease as mass increased and the surface area remained the same.

The results in **Figure 6c** shows the charge/mass linearly increased proportional to the number of mats in the stack. The charge/mass of stacked sample D (with five individual mats) was approximately double that of a single mat. Numerically this indicates that the measured charge per total mass increased over the single mat charge by about 25% for each additional mat in the stack. The increase in charge per mass indicates the

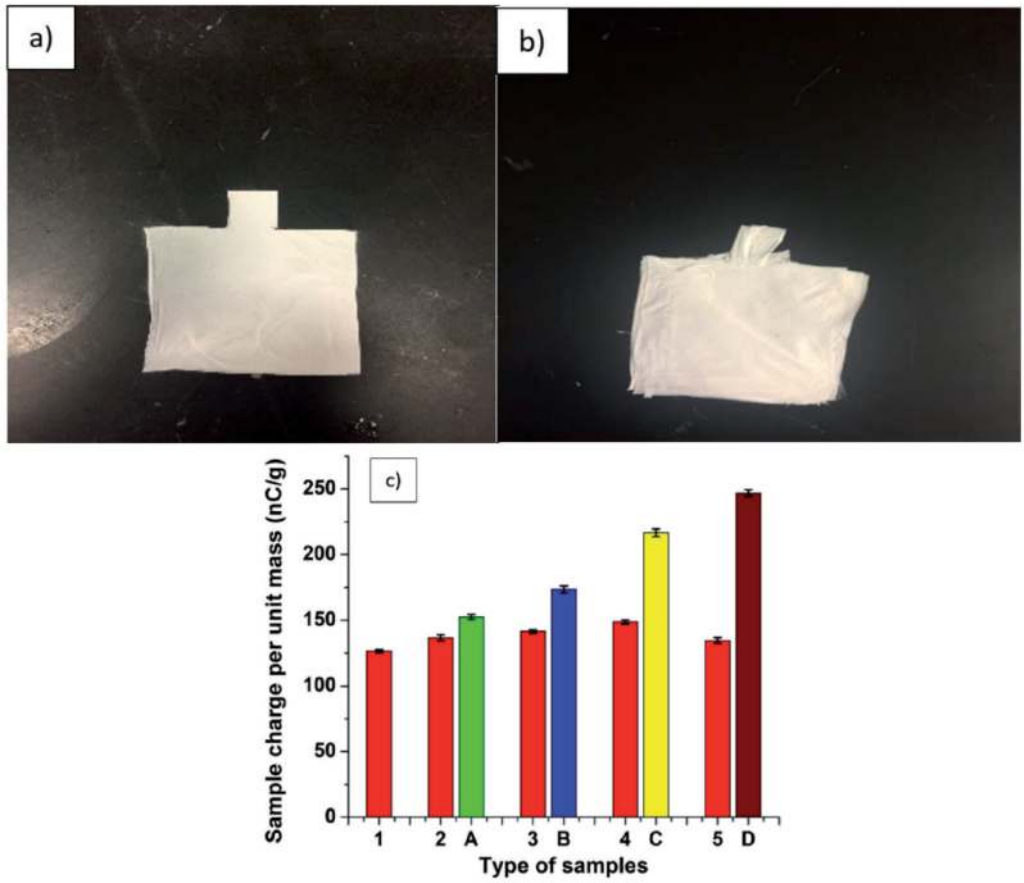

Figure 6.
(a) Photograph of example of a single fiber mat of size 4 × 4 cm with a 1 × 1 cm tab on one edge, (b) photograph of five mats stacked on top of each other. (c) Bar chart of charge/mass of various samples (1–5 = measured charge/mass of five individual samples) (a = charge of stacked mats 1 + 2, B = stacked mats 1 + 2 + 3, C = stacked mats 1 + 2 + 3 + 4, D = stacked mats 1 + 2 + 3 + 4 + 5). The error bars in (c) represent average of three charge measurements of same mats and error is one standard deviation.

bulk charge mechanism alone is unlikely. The increase in charge also strongly indicates that the measurement is not that of the charges on the external surfaces of the stacked mats assuming the charges do not migrate to the surface. Hence the mechanism is more complex. It is interesting to note that each subsequent mat added to the stack to linearly increased the measured charge by 25%. This gives the relationship

$$\frac{\left(C/M\right)}{\left(C_1/M_1\right)} = 0.25\left(\frac{M}{M_1}\right) + 0.75 \tag{1}$$

or

$$\frac{C}{C_1} = 0.25\left(\frac{M}{M_1}\right)^2 + 0.75\frac{M}{M_1} \tag{2}$$

where C is the measured charge of the stack and M is the mass of the stack. C_1 is the measured charge and M_1 is the mass of one mat. The ratio M / M_1 equals the number of mats in the stack. An interpretation of the meaning of the two terms on the right side of Eq. (2) is not apparent. Future experiments should be conducted by varying the surface areas of the mats to determine if the terms are related to area and possible migration of charges between the stacked mats.

3.2 Comparison of charge/mass of electrospun and polarized PVDF fibers and yarns

The plot in **Figure 7** compares the charges of the (a) as-spun mats and yarns, and (b) polarized mats and yarns. For comparison purposes the samples of polarized and nonpolarized mats and yarns are compared on equal mass basis. The labels A, B, C, D and E indicate the masses of fibers in the yarns and mats corresponding to 0.0058, 0.0124, 0.0196, 0.0278 and 0.0376 g respectively. The data reported in **Figure 7** are for electrospun mats of varying basis weights (not stacked layers of mats). For the given areas and masses of the mats the A, B, C, D and E mat samples correspond to 10, 20, 30, 40 and 50 g/m^2 basis weights.

In **Figure 7** the charges per mass of the mats were about 2 to 5 times the value for the yarns. The charge per mass of the as-spun and polarized mats increased as the mat mass increased with approximate slope of 17% (comparable to the 25% slope observed in the layered mats of **Figure 6**). Charges on the yarn samples did not vary as much with mass. Both the as-spun and polarized yarns tended to have a modest decrease in charge per mass as yarn mass increased. The difference in performance between the yarns and the mats is probably due to the way the yarn was folded to fit into the Faraday bucket. Increasing the mass of the yarn was obtained by increasing the length of the yarn hence the overall surface area per mass of the yarn was constant. But to fit the yarn into the Faraday bucket, the yarn was wound onto the U shaped metal wire which resulted in the first layers of the windings being covered by subsequent layers. Unlike the stacked fiber mats, the resulting charge/mass decreased with mass. This suggests that the measured charges per mass of the yarns were mostly proportional to the external area/mass ratio and may also give insight to the performance of the mats. This topic should be further explored in future work.

Figure 8 shows plots comparing the as-spun to polarized mats and yarns. The comparison of the mats in **Figure 8a** shows the polarized treatments only marginally increased the charges on the mats. This contrasts with the increases in charges reported in literature [6]. There were some differences between the treatments in this work compared to reference [6] such as the heat cycle in [6] was at a controlled ramp rate and the electrical polarization was maintained until the mat had completely cooled, while in this work the ramp rate was not controlled and the electrical polarization was for a shorter time period. It is possible, though not verified here,

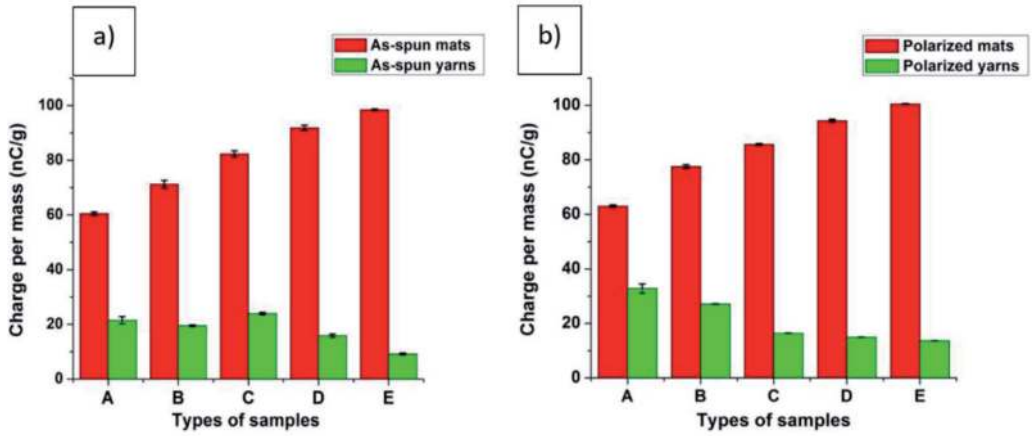

Figure 7.
Charge/mass plot for mats and yarns (a) as-spun, (b) polarized. The respective masses of the samples were a = 0.0058 g, B = 0.0124 g, C = 0.0196 g, D = 0.0278 g, and E = 0.0376 g.

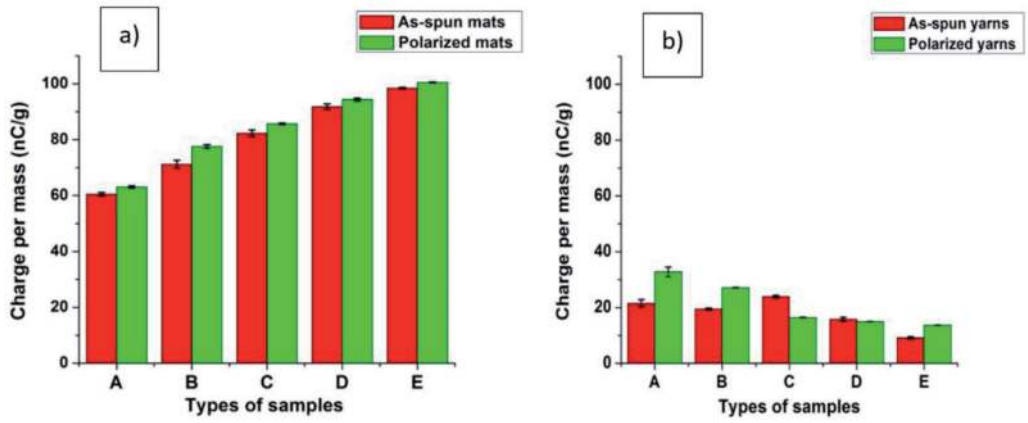

Figure 8.
Charge/mass plot for as-spun and polarized samples (a) Mats, (b) yarns the respective masses of the samples were a = 0.0058 g, B = 0.0124 g, C = 0.0196 g, D = 0.0278 g, and E = 0.0376 g.

that the beta phase content of the electrospun fibers was near its maximum in the as-spun fibers and hence the polarization treatment did not have much room to increase the beta phase content. This is left for future investigation.

The comparison of yarns in **Figure 8b** similarly show a small increase in the charge in most of the cases. Overall, the charges on the yarns did not change significantly with mass. The polarized samples A, B, and E showed greater charge compared to the as-spun samples while C and D showed less charge. These variations may be within experimental error possibly due to the hand winding of the yarns onto the U-shaped wire holder.

4. Conclusions

Polymer PVDF was electrospun to form fiber mats and continuous twisted yarns. Samples of the mats and yarns were polarized by stretching, heating and poling. The as-spun and polarized mats and fibers were measured for their charge via a Faraday bucket. The results showed the mats had significantly higher charge per mass than the yarns at the same mass. The measured charge per unit mass of the mats increased as the mass of the mat increased. The measured charge per mass of the yarns slightly decreased as mass increased. The polarization treatments used in this work did not significantly increase the charge of the mats and yarns. Charge measurements of stacked layers of mats suggest that the charge measured by the Faraday bucket is a complicated combination of surface area and bulk mass. Changing the basis weights of fiber mats (instead of stacking layers) gave similar trends suggesting the same mechanisms may apply to both stacked and directly spun mats. The nearly constant measured charges of the yarns suggest that the charge per mass may be related to the surface area per mass of the yarns.

Acknowledgements

This work was funded by Coalescence Filtration Fibers Consortium (CFNC): Parker Hannifin, Hollingsworth and Vose, and Donaldson. We acknowledge the assistance of technicians Steve Roberts and William Imes for fabrication and operation of the Faraday bucket.

Author details

Harshal Gade, Sreevalli Bokka and George G. Chase*
Department of Chemical, Biomolecular and Corrosion Engineering, The University of Akron, Akron, Ohio, United States of America

*Address all correspondence to: gchase@uakron.edu

References

[1] Damaraju SM, Wu S, Jaffe M, Arinzeh TL. Structural changes in PVDF fibers due to electrospinning and its effect on biological function. Biomedical Materials. 2013;8:045007. DOI: 10.1088/1748-6041/8/4/045007.

[2] Gaur A, Kumar C, Shukla R, Maiti P. Induced Piezoelectricity in Poly (vinylidene fluoride) Hybrid as Efficient Energy Harvester. Chemistry Select. 2017;2:8278-8287. DOI: 10.1002/slct.201701780.

[3] Li H-Y, Liu Y-L. Nafion-functionalized electrospun poly (vinylidene fluoride) (PVDF) nanofibers for high performance proton exchange membranes in fuel cells. Journal of Materials Chemistry A. 2014;2:3783-3793. DOI: 10.1039/C3TA14264G.

[4] Reneker DH, Chun I, Nanometre diameter fibres of polymer, produced by electrospinning. Nanotechnology. 1996;7:216-223.

[5] Gade H, Bokka S, Chase GG, Polarization treatments of electrospun PVDF fiber mats. Polymer. 2020;212,123152. DOI: 10.1016/j.polymer.2020.123152

[6] Lolla D, Lolla M, Abutaleb A, Renekar DH, Chase GG, Fabrication, polarization of electrospun polyvinylidene fluoride electret fibers and effect on capturing nanoscale solid aerosols. Materials. 2016;9:671-689. DOI: 10.3390/ma9080671.

[7] Lolla D, Pan L, Gade H, Chase GG, Functionalized Polyvinylidene Fluoride Electrospun Fibers and Applications, in Electrospinning Method Used to Create Functional Nanocomposite Films, T Tański editor, Intech Open Limited, London, UK, 2018; Volume 8.

[8] Collins L, Kilpatrick JI, Vlassiouk IV, Tseley A, Appl. Phys. Lett, 2014;104:133103.

[9] Du Q, Zhang Q, Wu Z, Ma J, Zhou J, Surface charge distribution on DC basin-type insulator. IEEE transactions on dielectrics and insulators. 2019;26(1): 17-25. DOI: 10.1109/TDEI.2018.007371.

[10] Takahashi T and Yoshita M, Scanning tunneling spectroscopy of-type GaAs under laser irradiation, Appl. Phys. Lett, 1997;70:2162.

[11] Fatihou A, Dascalescu L, Zouzou N, Neagoe MB, Measurement of Surface Potential of Non-uniformly Charged Insulating Materials Using a Non-contact Electrostatic Voltmeter, IEEE Transactions on Dielectrics and Electrical Insulation. 2016:23(4):2377-2384.

[12] Gade H, Parsa N, Chase GG, Renekar DH, Roberts OS, Charge measurement of electrospun polyvinylidene fluoride fibers using a custom-made Faraday bucket. Review of Scientific Instruments. 2020;91:075107. DOI: 10.1063/1.5142386

[13] Fredrick ER, Fibers, electrostatics, and filtration: a review of new technology. J Air Pollution Control Association. 1980:30(4), 426-431.

[14] Brown RC, Air Filtration, Pergamon Press, Oxford, 1993.

[15] Choi DY, An EJ, Jung S-H, Song DK, Oh YS, Lee HW, Lee HM, Al-Coated Conductive Fiber Filters for High-Efficiency Electrostatic Filtration: Effects of Electrical and Fiber Structural Properties. Scientific Reports. 2018: 8,5747.

[16] Romay FJ, Liu BY, Chae S-J. Experimental study of electrostatic capture mechanisms in commercial electret filters. Aerosol Sci. Technol. 1998:28:224-234.

[17] Walsh D, Stenhouse J, Parameters affecting the loading behavior and degradation of electrically active filter materials. Aerosol Sci. Technol. 1998:29: 419-432.

[18] Walsh D, Stenhouse J, The effect of particle size, charge, and composition on the loading characteristics of an electrically active fibrous filter material. J. Aerosol Sci. 1997:28:307-321.

[19] Wang S, Zhao X, Yin X, Yu J, Ding B, Electret Polyvinylidene Fluoride Nanofibers Hybridized by Polytetrafluoroethylene Nanoparticles for High-Efficiency Air Filtration. ACS Appl. Mater. Interfaces. 2016:8:23985-23994.

[20] Liu C, Hsu P-C, Lee H-W, Ye M, Zheng G, Liu N, Li W, Cui Y, Transparent air filter for high-efficiency PM2.5 capture. Nature Communications. 2015:6:6205.

[21] Khalid B, Bai X, Wei H, Huang Y, Wu H, Cui Y, Direct blow-spinning of nanofibers on window screen for highly efficient $PM_{2.5}$ removal. Nano Letters. 2017:17:1140-1148.

[22] Jing L, Shim K, Toe CY, Fang T, Zhao C, Amal R, Sun K-N, Kim JH, Ng YH, Electrospun Polyacrylonitrile–Ionic Liquid Nanofibers for Superior $PM_{2.5}$ Capture Capacity. ACS Applied Materials and Interfaces. 2016:8: 7030-7036.

[23] Li P, Zong Y, Zhang Y, Yang M, Zhang R, Li S, Wei F, In situ fabrication of depth-type hierarchical CNT/ quartz fiber filters for high efficiency filtration of sub-micron aerosols and high water repellency. Nanoscale 2013:5:3367-3372.

[24] Li, P., Wang, C., Zhang, Y. & Wei, F. Air Filtration in the Free Molecular Flow Regime: A Review of High-Efficiency Particulate Air Filters Based on Carbon Nanotubes. Small 2014:10:4543-4561.

[25] Varesano A, Carletto RA, Mazzuchetti G. Experimental investigations on the multi-jet electrospinning process. Journal of Materials Processing Technology. 2009;209:5178-5185. DOI : 10.1016/j. jmatprotec.2009.03.003

[26] Kim G, Cho YS, Kim WD. Stability analysis for multi-jets electrospinning process modified with a cylindrical electrode. European Polymer Journal. 2006;42:2031-2038. DOI : 10.1016/j. eurpolymj.2006.01.026

[27] Shuakat MN, Wang X, Lin T. Electrospinning of nanofiber yarns using novel ring collector, proceedings of the 2013 Fiber Society Spring conference, Fiber Society, Geelong, Australia, p. 238-239.

[28] Afifi AM, Nakano S, Yamane H, Kimura Y. Electrospinning of continuous aligning yarns with a funnel target. Macromolecular Material Engineering. 2010;295:660-665. DOI : 10.1002/mame.200900406.

[29] Teo W, Gopal R, Ramaseshan R, Fujihara K, Ramakrishna SA. dynamic liquid support system for a continuous electrospun yarn fabrication, polymer 2007;48:3400-3405. DOI : 10.1016/j. polymer.2007.04.044.

[30] Ali U, Zhou Y, Wang X, Lin T. Direct electrospinning of highly twisted. continuous nanofiber yarns. Journal of Textile Institute. 2012;103:1-9. DOI : 10.1080/00405000.2011.552254